CHEMICAL ENGINEERING TRANSACTIONS
VOL. 61, 2017
A publication of AIDIC
The Italian Association of Chemical Engineering
Online at www.aidic.it/cet
Guest Editors: Petar S Varbanov, Rongxin Su, Hon Loong Lam, Xia Liu, Jiří J Klemeš

ISBN 978-88-95608-51-8; **ISSN** 2283-9216
DOI: 10.3303/CET1761035

Effect of an Upstream Unconnected Bulge on Film Cooling

Qianqian Li[a], Jin Wang [a,b,*], Chunhua Min[a], Ke Tian[a], Liting Tian[a], Bengt Sundén[b]

[a]School of Energy and Environmental Engineering, Hebei University of Technology, Tianjin 300401, China
[b]Department of Energy Sciences, Division of Heat Transfer, Lund University, Lund SE-22100, Sweden
wjwcn00@163.com

Film cooling technology is commonly used in a cooling system of gas turbines. For different upstream bulge configurations, the unconnected and connected configurations were used to investigate the film cooling effectiveness and downstream dimensionless temperature distributions in this paper. Moreover, the effect of the blowing ratio was analyzed by using the computational fluid mechanics. The results show that a bulge configuration located upstream the film hole shows more uniform film cooling effectiveness, resulting in an enhancement of the lateral cooling effectiveness. The film cooling effectiveness for the unconnected bulge configuration slightly decreases along the centerline.

1. Introduction

To improve thermal efficiency, the inlet temperature of gas turbines show a rapidly increasing trend. Modern gas turbine engines operate under the high temperature of 1,800 – 2,000 K. Therefore, cooling techniques are needed to prevent the gas turbines from the high temperature. In order to investigate the fluid flow and heat transfer inside gas turbines, many researchers performed a large amount of experimental studies and numerical simulations. Koc et al. (2006) numerically investigated film cooling effectiveness of five different curved surface. Results show that under the optimal parameters condition, averaged film effectiveness depended on the blowing ratio and injection angle.
Na et al. (2007) studied influence of the upstream ramp on film cooling effectiveness at low blowing ratios. Based on cylindrical and fan-shaped holes, Barigozzi et al. (2007) performed experimental studied the effect of an upstream ramp, and the results showed that the fan-shaped hole case without a upstream ramp obtained the best film cooling effectiveness. In addition, Rallaband et al. (2011) analyzed the film cooling effectiveness on a flat plate by using the pressure sensitive paint technology, considering the effect of upstream steps with various height. They found that the upstream step had significant impact on the film cooling effectiveness near the film cooling hole. Rallaband et al. (2012) investigated interference of separated flows behind backward-facing step. Results indicated film-cooling effectiveness near the hole is improved due to the presence of the upstream step. Abdala et al. (2016) proposed novel upstream steps for improvement of the film cooling performance by using the software ANSYS CFX. The results showed that the curved step with less width (W/8) provided higher lateral film cooling effectiveness and lower heat transfer coefficient.
Upstream step becomes extremely urgent to protect the blade operated at the requirement of increasing the inlet temperature. Considering that influence of upstream steps has not been fully discussed, the film cooling effectiveness is numerically investigated at different blowing ratios in this study. In addition, the connected and unconnected bulge configurations are compared.

2. Description of Geometry

Three-dimensional (3D) models are used to investigate the effect of a bulge configuration on the film cooling effectiveness as shown in Figure 1. The computational domain is 80 d × 20 d × 4 d. The film hole has a diameter (d) of 8 mm. The outlet film hole is set to 30 d away from the outlet of the mainstream, and the vertical height of the jet hole is 2 d. An inclined angle (α) of 35° is adopted, and the distance between the bulge and the film cooling hole is 3 d. The height and width of bulge configurations are given in the first three columns of Table 1, and there are four kinds of unconnected distances listed in the last two columns.

Please cite this article as: Li Q., Wang J., Min C., Tian K., Tian L., Sundén B., 2017, Effect of an upstream unconnected bulge on film cooling, Chemical Engineering Transactions, 61, 223-228 DOI:10.3303/CET1761035

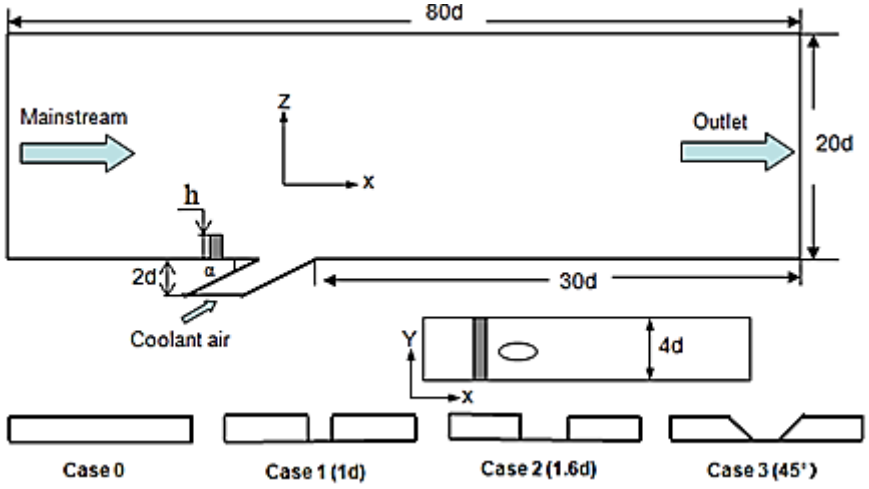

Figure 1: Computational domain and upstream configurations

Table 1: Dimensions of upstream configuration

Case	Bulge width	Bulge height	Unconnected length
Case0	0.3d	0.3d	0 d
Case1	0.3d	0.3d	1d
Case2	0.3d	0.3d	1.6d
Case3	0.3d	0.3d	45°

3. Governing equations

The governing equations of mass, momentum, energy, turbulent kinetic energy *k* and the turbulent dissipation rate ε are shown as follows:

$$\frac{\partial}{\partial x_i}(\rho u_i) = S_m \tag{1}$$

$$\frac{\partial}{\partial x_i}\left(\rho u_i u_j\right) = \rho \bar{g} - \frac{\partial P}{\partial x_j} + \frac{\partial}{\partial x_i}\left(\tau_{ij} - \rho\overline{u_i' u_j'}\right) + F_j \tag{2}$$

$$\frac{\partial}{\partial x_i}\left(\rho c_p u_i T\right) = \frac{\partial}{\partial x_i}\left(\lambda \frac{\partial T}{\partial x_i} - \rho c_p \overline{u_i' T'}\right) + \left|\mu\Phi + S_h\right| \tag{3}$$

$$\frac{\partial}{\partial x_i}(\rho k u_i) = \frac{\partial}{\partial x_i}\left(\alpha_k \mu_{eff} \frac{\partial k}{\partial x_j}\right) + G_k + G_b - \rho\varepsilon - Y_M + S_k \tag{4}$$

$$\frac{\partial}{\partial x_i}(\rho \varepsilon u_i) = \frac{\partial}{\partial x_j}\left(\alpha_\varepsilon \mu_{eff} \frac{\partial \varepsilon}{\partial x_j}\right) + C_{1\varepsilon}\frac{\varepsilon}{k}(G_k + C_{3\varepsilon}G_b) - C_{2\varepsilon}\rho\frac{\varepsilon^2}{k} - R_\varepsilon + S_\varepsilon \tag{5}$$

More details can be found in ref. (Wilcox D.C., 2006).

4. Boundary conditions

Boundary conditions are given in Table 2. Both the mainstream and the coolant flow are assumed to be air, and the inlet temperatures are 400 K and 300 K. The mainstream velocity is 40 m/s, and different blowing ratios (M) are adopted, including 0.25, 0.5, 0.75 and 1. The blowing ratio M is defined as $M=(\rho u)_c/(\rho u)_g$, and the subscript *c* and *g* are represent the coolant flow and the mainstream gas.

Table 2: Boundary conditions

Zone	Type	Value
Mainstream	Velocity-inlet	40 m/s, 400 K
Coolant air	Velocity-inlet	300 K
Outlet	Pressure-outlet	101,325 Pa
Side walls	Symmetry	/
Other walls	No-slip	/

5. Meshes and model validation

The velocity and pressure coupling adopted SIMPLE algorithm, and RNG k-ε turbulence models were used in this paper. Both structured and unstructured grids are used for all the cases. The grids near both the jet hole and the bottom wall are denser than those near both the outlet and the inlet. This is because the fluid flow in these zones is relatively complicated. The grid density decreases downstream the wall. All the results are obtained by using the ANSYS FLUENT 16.0. More than 3,000 iterations are necessary to reach the converged results.
The concerned values are also monitored, including average values of the bottom wall temperature, the velocities at the inlet and the outlet of the mainstream. It can be supposed to be the end of calculations when the residual less than10^{-5}. The nearest wall cell had a value of y+ = 2.62. Four different meshes (0.28, 0.53, 1.02 and 1.85 million) were used to analyse the grid independence as shown in Figure 2. Considering overlapped values for the cases with above 0.53 M cells, 0.53 M of grids was finally adopted in this paper.

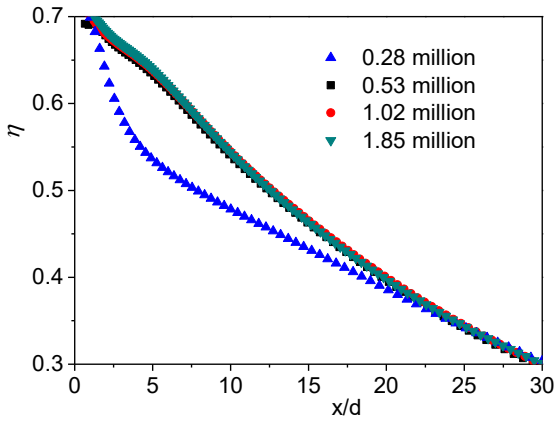

Figure 2: Grid independence

Compared to the results (Li and Wang, 2006), the previous results (Wang et al., 2016) have almost overlapped values for cases with above 0.53 M meshes as shown in Fig. 3. The present results are obtained by using the same method and similar boundary conditions.

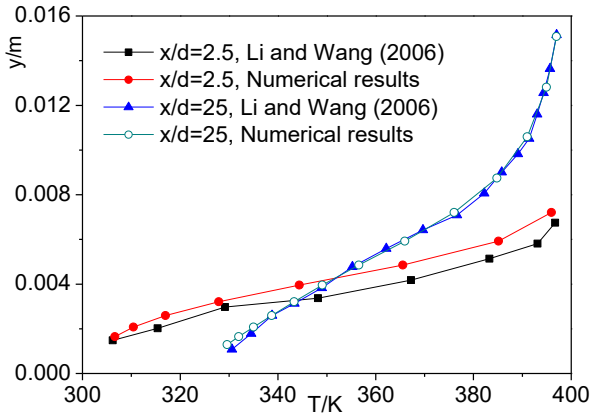

Figure 3: Model validation (Wang et al., 2016)

6. Results and Discussion

The film cooling effectiveness η is defined as $\eta=(T_g-T_{aw})/(T_g-T_c)$, and the dimensionless temperature θ is defined as $\theta=(T_g-T_{la})/(T_g-T_c)$. T_g, T_{aw}, T_c, and T_{la} are the mainstream gas temperature, the adiabatic wall temperature, the coolant flow temperature and the local air temperature.

Figure 4 shows dimensionless temperature on the middle section at the blowing ratio of 1. High film cooling effectiveness appears downstream the wall (dotted circle). Compared with the connected bulge configuration, the film cooling effectiveness is obviously improved for the case with the unconnected bulge configuration. The case with unconnected bulge configuration obtains a higher cooling performance. With the increase of unconnected distance, the film cooling ability is enhanced significantly downstream the wall, while the core of the high effectiveness zone is approaching to the location of the film hole.

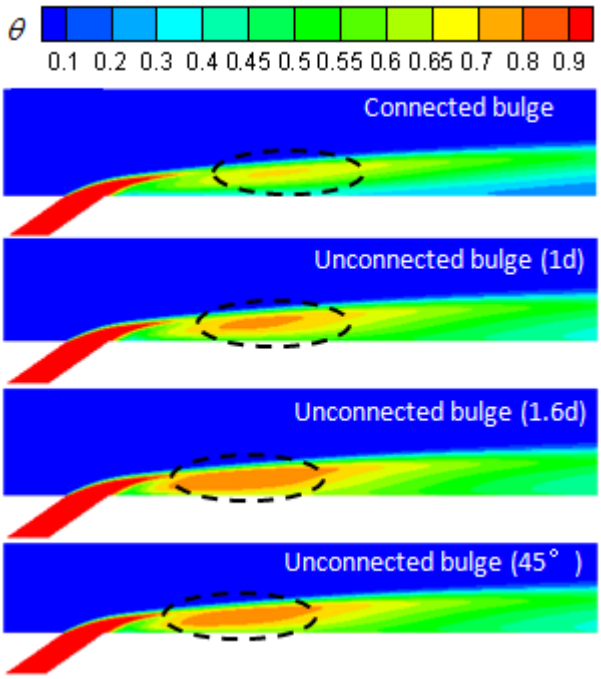

Figure 4: Dimensionless temperature on the middle section with M = 1

The wall film cooling effectiveness distribution with the blowing ratio of 0.25 are shown in Figure 5. Compared with connected bulge configuration, the case with 1 d unconnected bulge configuration obtains a higher lateral cooling effectiveness. Although the influenced scope of the coolant jet decreases downstream the wall, the lateral film cooling effectiveness is improved remarkably, and the coverage area near the film cooling hole enlarges obviously.

To analyse the effect of unconnected bulge configuration on the film cooling effectiveness, Figure 6 quantitatively presents the cooling effectiveness on the wall centreline with the low blowing. It is found that the film cooling effectiveness for the unconnected bulge case (1 d and 45 degree) is slightly lower than for the connected bulge case within the range of $10 < x/d < 30$. Compared with the connected bulge case, the case with unconnected bulge shows more free space of the coolant air to extend laterally. It indicates that a portion of the cooling performance downstream the centreline is sacrificed for an improvement of the lateral cooling effectiveness.

Figure 7 shows the lateral film cooling effectiveness at x = 5d with blowing ratio of 0.25. It is found that the film cooling effectiveness for the unconnected bulge case is higher than for the connected bulge case in the entire range. The case with the 1d unconnected bulge shows higher film cooling effectiveness near the centerline. This is because the mainstream is lifted up by the bulge configuration and the suppression from the mainstream to the coolant air is weakened. The coolant air spreads from the central region to both sides of the bulge. Therefore, the film cooling effectiveness for the unconnected bulge configuration is significantly improved both in the lateral direction and downstream the wall.

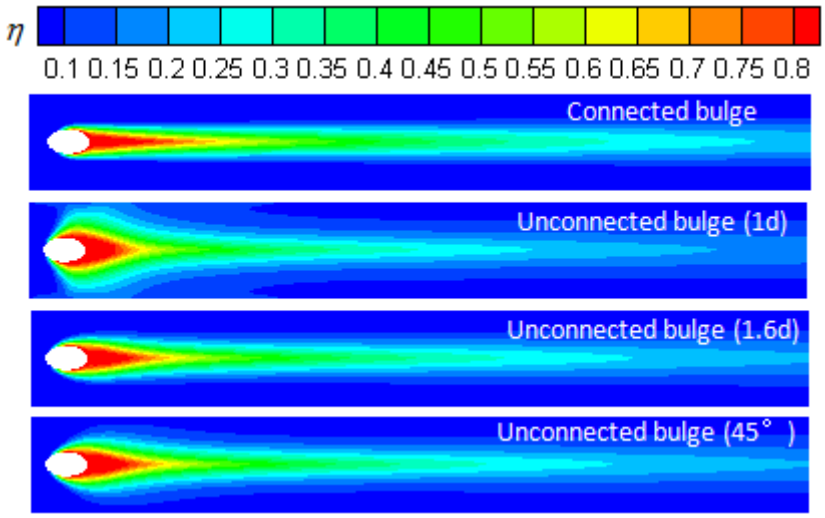

Figure 5: Wall film cooling effectiveness distribution with M=0.25

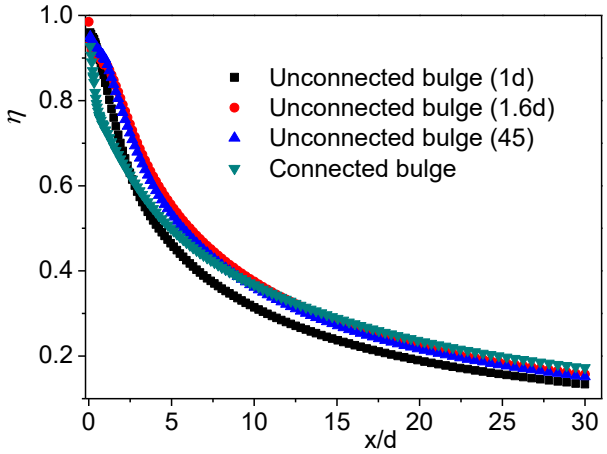

Figure 6: Film cooling effectiveness on the wall centreline with M = 0.25

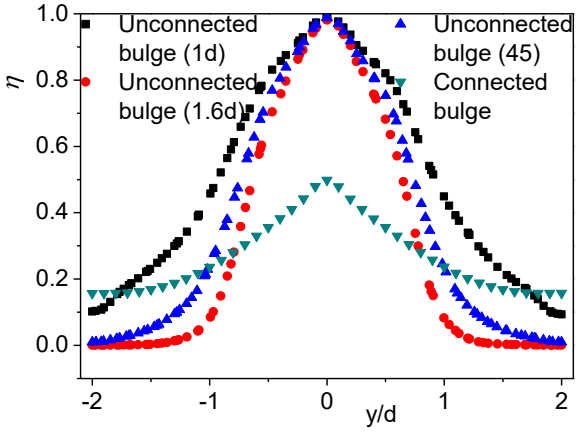

Figure 7: Lateral film cooling effectiveness at x/d=5 with M=0.25

For the configuration with unconnected distance of 1.6 d, the film cooling effectiveness on the wall centreline is quantitatively investigated as shown in Figure 8. For the case with blowing ratio under 0.5, the results show that the film cooling effectiveness increases apparently with increasing the blow ratio. At the position of x = 15 d, the film cooling effectiveness with the blowing ratio of 0.5 increases by 51.28 % compared to that with the

blowing ratio of 0.25. For the case with the high blowing ratio, the film cooling effectiveness near the film hole is reduced. The film cooling effectiveness downstream the wall slightly decreases with the increasing the blow ratio.

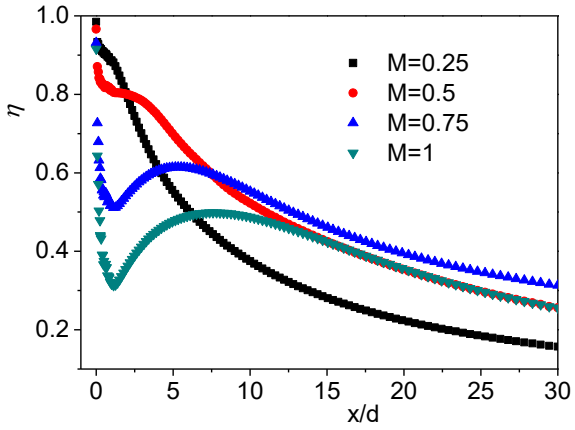

Figure 8: Film cooling effectiveness on the wall centreline with different flowing ratios

7. Conclusions

Connected and unconnected bulge configurations were positioned upstream the film hole. A comparison of various unconnected configurations is conducted numerically, and the film cooling effectiveness distributions were investigated in this paper. The main findings can be summarised as follows: the upstream bulge configuration increases the mixing distance between the mainstream and the coolant air; compared with connected bulge configuration, the unconnected bulge case obtains a more uniform temperature distribution and a lower thermal stress concentration. Film cooling effectiveness for the connected bulge case is reduced downstream the wall (x/d 〉 10). The film cooling effectiveness on the centreline significantly increases in the range of x/d < 10. An unconnected bulge configuration provides a weaker penetration from the coolant air to the mainstream.

Acknowledgments

This work is supported by the National Natural Science Foundation of China (Grant No. 51606059) and the Natural Science Foundation of Hebei Province (Grant No. E2016202266).

Reference

Abdala A.M.M., Elwekeel F.N.M., 2016, An Influence of Novel Upstream Steps on Film Cooling Performance, International Journal of Heat and Mass Transfer, 93, 86-96

Barigozzi G., Franchini G., Perdichizzi A., 2007, The Effect of an Upstream Ramp on Cylindrical and Fan-Shaped Hole Film Cooling: Part I - Aerodynamic Results, ASME Turbo Expo 2007: Power for Land, Sea, and Air, Vol 4, Montreal, Canada, 105-113, doi:10.1115/GT2007-27077

Koc I., Parmaksizoglu C., Cakan M., 2006, Numerical Investigation of Film Cooling Effectiveness on the Curved Surface, Energy Conversion and Management, 47(9-10), 1231-1246.

Li X.C., Wang T., 2006, Simulation of Film Cooling Enhancement with Mist Injection, ASME Journal of Heat Transfer, 128(6), 509-519.

Na S., Shih T.I.P., 2007, Increasing Adiabatic Film-cooling Effectiveness by Using an Upstream Ramp, ASME Journal of Heat Transfer, 129(4), 931-938.

Rallabandi A.P., Grizzle J., Han J.C.,2011, Effect of Upstream Step on Flat Plate Film Cooling Effectiveness Using PSP, Journal of Turbomachinery, 133(4), 599-609.

Terekhov V.I., Smul'skii Y.I., Sharov K.A., 2012, Interference of Separated Flows Behind Backward-facing Step in the Presence of Passive Control, Technical Physics Letters, 38(2), 125-128.

Wang J., Cui P., Sundén B., Vujanović M., 2016, Effects of Deposition Height and Width on Film Cooling, Numerical Heat Transfer, Part A: Applications, 70(6), 673-687

Wilcox D.C., 2006, Turbulence Modeling for CFD, DCW Industries Inc., California, USA, 522 ps, ISBN: 987-1-928729-08-2.